Journal of Applied Mechanics and Technical Physics, Vol. 48, No. 2, pp. 159–165, 2007

INVESTIGATION OF AERODYNAMIC CHARACTERISTICS OF A HYPERSONIC FLOW AROUND BODIES OF REVOLUTION WITH A PERMEABLE TIP

N. I. Sidnyaev

UDC 629.136

Results of experimental investigations of aerodynamic characteristics of models of high-velocity flying vehicles consisting of a combination of a blunt cone, a cylinder, and a conical tail fin are presented. The model forebody is cooled by porous blowing. The choice of such a configuration is determined by the necessity of optimizing the arrangement of high-velocity flying vehicles on the launcher and their aerodynamic characteristics under conditions of intense surface mass transfer (decrease in drag and heat transfer and increase in static and dynamic stability).

Key words: *aerodynamic characteristics, mass transfer, heat transfer, supersonic, dynamic stability, moment.*

The development of reliable means of thermal protection of flying vehicles moving with high supersonic velocities in dense atmospheric layers involves many difficult tasks, which include the problem of mass transfer on the vehicle surface. There are many methods of active and passive thermal protection in aviation and rocket engineering practice, which is caused by the variety of configurations of flying vehicles and specific conditions of their atmospheric flight [1–3]. An important problem in the development and design of advanced high-velocity flying vehicles is the allowance for the effect of intensity of gas injection into the boundary layer and the distribution of injection over the body surface on local and integral characteristics of flying vehicles [4–6]. Passive methods of thermal protection based on the use of ablative thermoprotective coatings are currently most popular [1, 6]. A significant drawback of these methods is a change in the original geometry of flying vehicles and, correspondingly, their aerodynamic characteristics in the course of flight, which alters ballistic parameters.

Numerous studies, including those performed recently, allow us to conclude that systems of active thermal protection of flying vehicles by forced injection of a coolant into the boundary layer are highly effective and promising [1, 2]. An important advantage of such systems is an unchanged geometric shape of the vehicle and, hence, its aerodynamic characteristics up to the final point of the flight trajectory.

Depending of flight conditions, properties of thermoprotective coatings, or physical and chemical properties of the coolant, the intensity of surface mass transfer (gas injection), which is usually characterized by the dimensionless parameter of injection $\overline{\rho_w v_w} = \rho_w v_w/(\rho_\infty u_\infty)$, may vary within wide limits (ρ_w, v_w and ρ_∞, u_∞ are the densities and velocities of the injected gas and incoming flow, respectively).

The results of experiments and in-flight tests show that the motion of high-velocity flying vehicles in dense atmospheric layers involves flow regimes corresponding both to weak injection of the gas into the boundary layer and to intense surface mass transfer [1–3, 5, 6]. The following flow regimes can be formed on complex-shaped flying vehicles on particular segments of the flight trajectory because of significantly different conditions of the flow around various elements of the body and the use of different materials of thermoprotective coatings: weak injection without displacement of the boundary layer (Fig. 1a), intense injection with boundary-layer displacement (Fig. 1b),

Bauman Moscow State Technical University, Moscow 105005; Sidn_ni@mail.ru. Translated from Prikladnaya Mekhanika i Tekhnicheskaya Fizika, Vol. 48, No. 2, pp. 19–26, March–April, 2007. Original article submitted July 1, 2004; revision submitted May 4, 2006.

0021-8944/07/4802-0159 © 2007 Springer Science + Business Media, Inc.

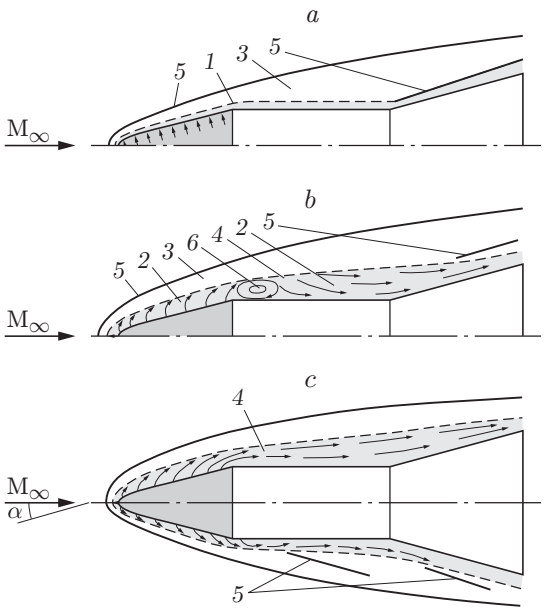

Fig. 1. Flow patterns around a complex-shaped body with a permeable conical nose part: (a) weak injection; (b) intense injection; (c) flow at an angle of attack; 1) boundary layer; 2) injection zone; 3) external flow region; 4) viscous mixing region; 5) shock waves; 6) stagnant zone.

and a steady flow near a spherically blunted body with a permeable tip at incidence at $M_\infty = 6$ and $\gamma_\infty = 1.4$ in the case of intense injection from the surface of a permeable conical part of the model (Fig. 1c).

The aerodynamic characteristics of complex-shaped bodies of revolution were determined in experiments with a flying vehicle model, which was a combination of a spherically blunted conical tip, a cylindrical central part, and a conical tail fin (Fig. 1). The permeable shell of the conical part of the model was manufactured by sintering [2] the powders of tin bronze (the Sn content was approximately equal to 9%) with free loading of powers into the moulds. The sintering technique and the methods used to study the coating characteristics (porosity and permeability) were described in detail in [1, 2]. The mould for sintering of porous shells was made of doped steel.

The model for studying the effect of distributed gas injection from the conical part of the model into the boundary layer on aerodynamic characteristics consisted of three elements: a spherically blunted cone 0.07 m long with a half-angle of 14°, a cylindrical part 0.08 m long, and a conical tail fin 0.075 m long with a cone half-angle equal to 11°30′. The dimensionless bluntness of the nose part was $\bar{R}_0 = R_0/R_{\text{mid}} = 0.2$. The mid-section radius was $R_{\text{mid}} = 0.04$ m, and the total length of the model was $b = 0.225$ m. The bottom part of the model had a soldered flange for reduction sleeves used to fix the model on the aerodynamic balance. The porous shell of the conical part of the model was produced by sintering bronze powders with the particle size ranging from 50 to 63 μm. The permeability of the shell was rather low, and the local deviation of the specific mass flow of the gas through the shell $\overline{\rho_w v_w}$ from its mean value was less than 4%. The mass flow of the gas through the porous shell was proportional to the pressure difference on the wall; owing to the low permeability of the shell, it was necessary to substantially increase the pressure inside the shell (up to 3 MPa) to ensure a required intensity of injection. This procedure, in turn, significantly alleviated the effect of the external pressure distribution over the body on uniformity of surface mass transfer. The aerodynamic characteristics of the models were studied in a supersonic wind tunnel at a Mach number $M_\infty = 6$. The free-stream stagnation temperature was $T_0 = 493$ K, the pressure in the settling chamber was $P_0 = 3.9$ MPa, and the Reynolds number per meter was $\text{Re}_\infty = 3.8 \cdot 10^7$ m^{-1}. The angle of attack was varied within $\alpha = 0$–$15°$, and the Strouhal number under these test conditions was $\text{Sh} = 2.9 \cdot 10^{-3}$–$3.13 \cdot 10^{-3}$.

The reference area and the reference length scale in calculating the aerodynamic coefficients were the mid-section area of the model S and the model length b. The temperature of the injected gas $T_w = 293$ K was assumed to be equal to the temperature of air inside the model. The flow in the shock layer near the examined model was close to an equilibrium flow with an effective ratio of specific heats equal to 1.3884 in the neighborhood of the stagnation point.

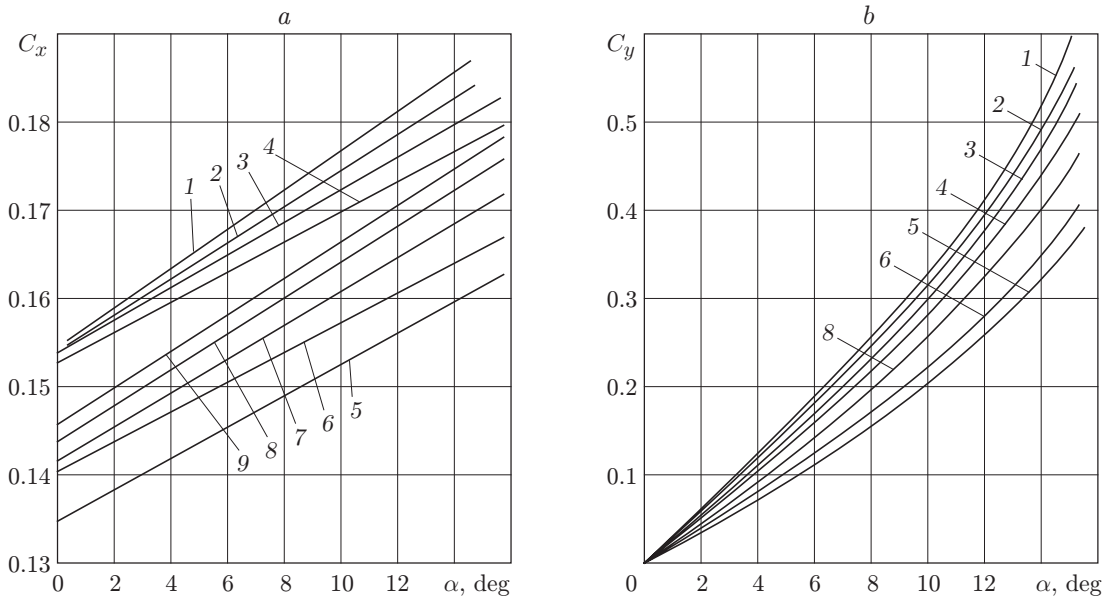

Fig. 2. Coefficients C_x (a) and C_y (b) versus the angle of attack for $\overline{\rho_w v_w} = 0$ (1), 1.2 (2), 2.8 (3), 4.6 (4), 6.2 (5), 7.8 (6), 8.8 (7), 10.4 (8), and 12.6% (9).

The model for studying the aerodynamic characteristics was fixed in a mechanism that inserted the model into the flow after the hypersonic wind tunnel was started and a prescribed flow regime was reached. For the present test series, the mechanism was designed so that the model was fixed when it was inserted into the flow and brought out of the flow. When the model was inside the wind-tunnel flow, its oscillations were periodically excited, which were registered simultaneously with time recording on an oscillograph.

Distributed injection of the gas through the surface of the conical part of the model, even if the injection intensity is low, provides an earlier laminar–turbulent transition of the boundary layer with a corresponding change in the flow structure (see Figs. 1a and 1b). Because of the tripping effect of the injected gas, there is a small increase in drag, if the dimensionless mass flow of the injected gas $\overline{\rho_w v_w}$ does not exceed a critical value [4, 6]. If the model is mounted at an angle of attack, the lift force coefficient is a nonmonotonic function of the injection intensity (Fig. 2). In this case, the total drag slightly decreases at $\overline{\rho_w v_w} \leqslant 7\%$, which exerts a significant effect on the lift-to-drag ratio [6]. At $\overline{\rho_w v_w} > 7\%$, the drag starts increasing (Fig. 3) because of an increase in the effective thickness of the cone (see Fig. 1b) and pressure redistribution [5, 6]. As the injection intensity increases, the boundary layer is displaced from the body surface, and a layer of the injected gas is formed near the latter, which joins the impermeable cylindrical surface of the model forebody with formation of a stagnant zone. The shock wave disappears, and the stand-off distance between the body surface and the shock wave somewhat increases, which is due to variation of the shape of the "effective" body (see Fig. 1b). As the injection intensity increases, these features become even more pronounced. The qualitative patterns of the flow around the models are obtained by processing Schlieren pictures obtained by a shadowgraph.

Equilibrium of a flying vehicle is determined by its static stability. To analyze the static stability, we performed wind-tunnel experiments with an air flow around a flying vehicle model fixed at the center of mass with a possibility of rotating around the latter.

The pitching moment M_z was determined with respect to the point in the plane of symmetry $\bar{x} = x/b = 0.675$. In the case of gas injection, the center of pressure moved upstream at a distance corresponding to 3–5% of the length of the body of revolution. The results of our study are plotted in Fig. 4. The coefficient $m_z = M_z/(qSb)$ was calculated with respect to the nose part of the body of revolution (Fig. 5). The criterion of static stability δ was assumed to be the dimensionless difference of the distances from the model tip to the center of mass $x_{\text{c.m.}}$ and center of pressure $x_{\text{c.p.}}$: $\delta = (x_{\text{c.m.}} - x_{\text{c.p.}})/b = \bar{x}_{\text{c.m.}} - \bar{x}_{\text{c.p.}}$.

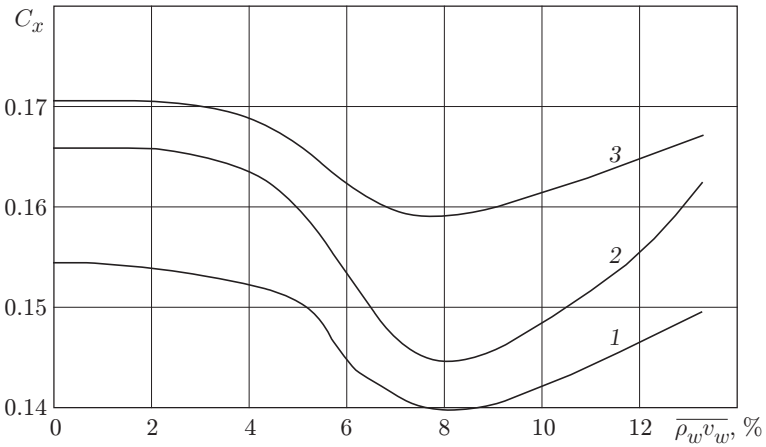

Fig. 3. Coefficient C_x versus the injection intensity for $\alpha = 0$ (1), 6 (2), and 12° (3).

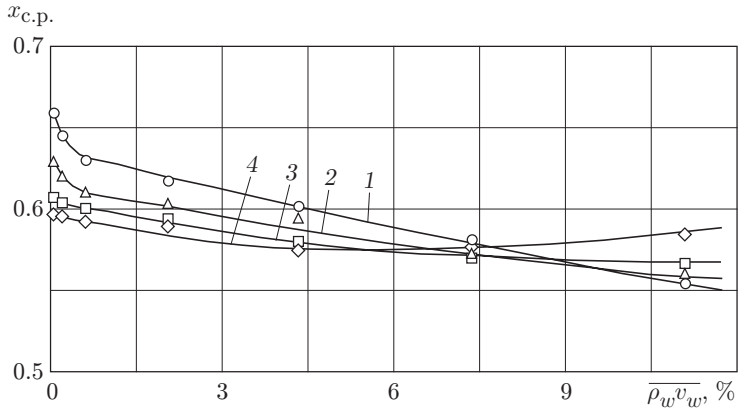

Fig. 4. Dependence of $x_{\text{c.p.}}$ on the injection intensity for $\alpha = 2$ (1), 6 (2), 10 (3), and 14° (4).

To determine the influence of the aerodynamic characteristics (derivatives of stability) on stability of motion of a flying vehicle with surface mass transfer, we performed tests with free oscillations [7]. In these tests, the model was mounted onto a sting that could perform free oscillations. Being pushed out of equilibrium, the model performed gradually decaying oscillations under the action of elastic elements of the sting, and the results were recorded by a loop oscillograph. The oscillogram also contained a time indication, which allowed us to determine the period of model oscillations.

The experiments were performed at a constant velocity and different angles of attack [8]. Based on the slope of the tangent lines to the curves $C_y = f(\alpha)$ and $m_z = f(\alpha)$, we determined the derivatives C_y^α and m_z^α. In addition, based on experimental data, we found the coefficients C_{y_0} and m_{z_0} (with respect to the model tip) [8].

The method of small oscillations made it possible to determine all coefficients of rotational derivatives, which enter, for instance, the expressions for the lift force Y and pitching moment M_z. The essence of this method is as follows. Small rotational harmonic oscillations (around the Oz axis) are applied to the model tested in the wind tunnel, and the aerodynamic force and moment are measured. In the case of free oscillations [7], the angular frequency χ is determined by the relation

$$\chi = \sqrt{m^2 - n^2} = 2\pi/T,$$

where

$$2n = \frac{\mu^2 - (m_z^{\omega_z} + m_z^{\dot\alpha})qSb^2/u}{J_z'}, \qquad m^2 = \frac{k^2 - m_z^\alpha qSb}{J_z'}, \qquad J_z' = J_z - m_z^{\dot\omega_z}\rho S\,\frac{b^3}{2},$$

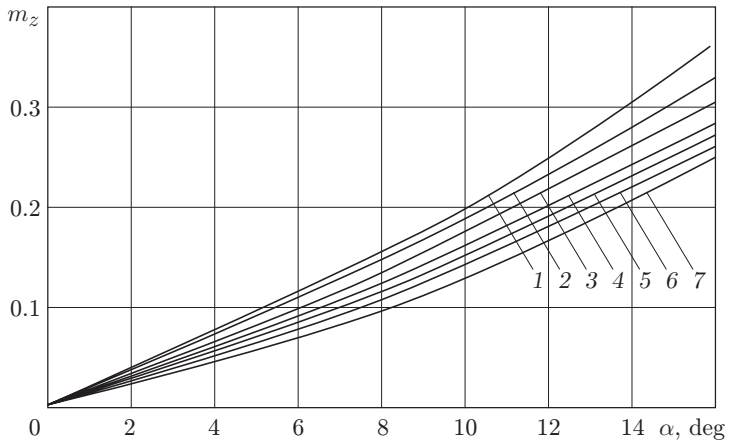

Fig. 5. Pitching moment coefficient versus the angle of attack for $\overline{\rho_w v_w} = 0$ (1), 1.4 (2), 2.8 (3), 4.6 (4), 6.2 (5), 8.4 (6), and 12.2% (7).

k^2 is the elasticity of the measurement system, expressed in terms of elasticity of the balance beams, J_z is the reduced moment of inertia, and $m_z^{\dot\alpha}$ and $m_z^{\dot\omega_z}$ are the coefficients at rotational derivatives of streamwise damping.

The experimental results suggest that the initial amplitude of oscillations θ_1^0 and any other ith amplitude θ_1^i are related as

$$n = \frac{1}{iT} \ln \frac{\theta_1^0}{\theta_1^i}.$$

This formula allows us to determine the coefficient n, based on the oscillation period and on the ratio of the amplitudes. Knowing the values of n and χ, we can find m. The condition providing oscillatory motion of the model for small values of $m_z^{\dot\omega_z}\rho Sb^3/2$, as compared with J_z, is written as $k^2 - m_z^\alpha qSb > 0$ [7]. This inequality is valid for statically stable models [8].

To ensure such motion, the model was mounted on a dynamic balance on a special sting, which allowed oscillations around the Oz axis. For example, in the case of model oscillations around the Oz axis with the quantity $m_z^{\dot\omega_z}\rho Sb^3/2$ being neglected because of the low density of the flow, which is small in airflow tests as compared with the reduced moment of inertia J_z [7], the sum of the coefficients of rotational derivatives $m_z^{\dot\alpha} + m_z^{\omega_z}$ is found by the formula

$$m_z^{\dot\alpha} + m_z^{\omega_z} = (\mu^2 - 2J_z n)u/(qSb^2).$$

Here μ^2 is the friction coefficient in elements of the sting for free oscillations. The damping coefficient n and the reduced moment of inertia of the system J_z are determined in the absence of the flow. The friction coefficient μ^2 in the balance sting is obtained by replacing the model by an equivalent load and finding the damping coefficient of the system n_1: $n = n_a + n_1$ (n_a is the damping coefficient of the balance in the airflow; for $u = 0$, we have $n_a = 0$ and $n = n_1$) [7]. The value of μ^2 is found from the relation

$$\mu^2 = 2n_1 J_{z_1},$$

where J_{z_1} is the reduced moment of inertia of the balance with the equivalent load [7]. In this case, we have

$$m_z^{\dot\alpha} + m_z^{\omega_z} = 2u(n_1 J_{z_1} - nJ_z)/(qSb^2).$$

In determining μ^2, the equivalent load was chosen so that its mass and position of the center of mass with respect to the axis of revolution corresponded to the mass and position of the center of mass of the model. Friction of the load on air during oscillations was ignored as being very small. The calibrations showed that the quantity μ^2 is very small and almost independent of the load mass. Thus, wind-tunnel tests allow us to determine the sum of the coefficients $m_z^{\dot\alpha} + m_z^{\omega_z}$ rather than the coefficient $m_z^{\omega_z}$. Figure 6 shows the coefficient of the damping moment $m_z^{\dot\alpha} + m_z^{\omega_z}$ as a function of the injection intensity (the root-mean-square error is within 6%).

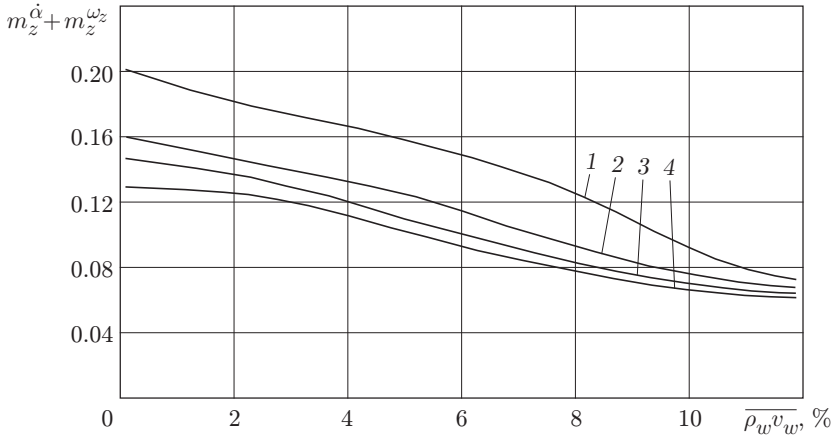

Fig. 6. Sum of the coefficients of rotational derivatives versus the intensity of injection from the conical part of the model for $\alpha = 0$ (1), 2 (2), 4 (3), and 6° (4).

The root-mean-square errors of the aerodynamic coefficients have the following form:

$$\sigma_{C_x} = \sqrt{\left(\frac{\sigma_x}{qS}\right)^2 + (C_x\varepsilon_q)^2}, \quad \sigma_{Cy} = \sqrt{\left(\frac{\sigma_y}{qS}\right)^2 + (C_y\varepsilon_q)^2}, \quad \sigma_{m_z} = \sqrt{\left(\frac{\sigma_{M_z}}{qSL}\right)^2 + (m_z\varepsilon_q)^2}.$$

Note that the relative root-mean-square error of determining the injection intensity is 2.64%.

The calculations yield the following dimensionless root-mean-square errors of determining the aerodynamic loads and coefficients for the examined bodies: $\varepsilon_x = 1.38\%$, $\varepsilon_y = 1.11\%$, $\varepsilon_{M_z} = 1.2\%$, $\varepsilon_{C_x} = 1.93\%$, $\varepsilon_{C_y} = 2.17\%$, and $\varepsilon_{m_z} = 3.28\%$.

Gas injection from the conical part of the blunt cone–cylinder model exerts a significant effect on the aerodynamic characteristics. The presence of a thick layer of the injected gas on the body surface leads to pressure redistribution and, correspondingly, alters the aerodynamic characteristics of the body. The dependence $C_x(\rho_w v_w)$ is nonmonotonic. The drag decreases if the injection intensity is fairly low ($\overline{\rho_w v_w} \leqslant 7\%$) and increases if $\overline{\rho_w v_w} > 7\%$.

In the case of an asymmetric flow around the body under intense injection (owing to gas overflow), the difference in pressures on the windward and leeward sides becomes smaller (see Fig. 1c), which reduces the normal force coefficient and, correspondingly, the lift-to-drag ratio. The injection intensity $\overline{\rho_w v_w} \geqslant 6\%$ yields a lower lift-to-drag ratio because of an increase in drag. The center of pressure is shifted upstream (the static stability decreases); the magnitude of this shift depends on the injection intensity and on the angle of attack and turns out to reach the greatest values in the range of low angles of attack. An increase in the angle of attack is accompanied by a monotonic decrease in the coefficients of the pitching moment m_z and center of pressure $x_{\text{c.p.}}$. For $\overline{\rho_w v_w} \leqslant 7\%$, the center of pressure is shifted upstream with increasing angle of attack, and the value of $x_{\text{c.p.}}$ remains lower than the value of this coefficient in the absence of injection.

In the entire examined ranges of injection parameters and angles of attack, distributed injection of the gas leads to a decrease in the damping coefficient $m_z^{\dot\alpha} + m_z^{\omega_z}$. The effect of the angle of attack on the dynamic derivative of stability depends on the alignment of the oscillation axis. An upstream shift of the oscillation axis increases dynamic stability of the blunt body of revolution. A significant decrease in dynamic stability with increasing angle of attack and injection intensity is observed in experiments only for $\overline{\rho_w v_w} \leqslant 10\%$.

It should be noted that an analysis of derivatives of aerodynamic moments in terms of the angle of attack α allows one to find whether a body possesses static stability of a certain kind in certain regions of trajectory motion under conditions of intense surface mass transfer.

REFERENCES

1. N. I. Sidnyaev, V. T. Kalugin, and A. Yu. Lutsenko, *Scientific Fundamentals of Technologies of the 21st Century* [in Russian], Énergomash, Moscow (2000).
2. N. I. Sidnyaev, "Mathematical modeling of distributed intense surface mass transfer in the flow around hypersonic flying vehicle models," *Vestn. Mosk. Gos. Tekh. Univ., Ser. Estestv. Nauki*, No. 2, 54–63 (2001).
3. N. I. Sidnyaev, "Method of numerical calculation of a supersonic flow around an oscillating axisymmetric body of revolution under conditions of intense surface mass transfer," *Vestn. Mosk. Gos. Tekh. Univ., Ser. Estestv. Nauki*, No. 1, 71–87 (2003).
4. N. I. Sidnyaev, "Method for studying the coefficients of rotational derivatives of the aerodynamic moment of a cone with surface mass transfer," *Izv. Vyssh. Uchebn. Zaved., Aviats. Tekh.*, No. 2, 30–33 (2004).
5. N. I. Sidnyaev, "Method for calculating an unsteady flow around a body of revolution with surface mass transfer by parabolized Navier–Stokes equations," *Mat. Model.*, **16**, No. 5, 55–65 (2004).
6. N. I. Sidnyaev, "Review of methods for studying a hypersonic flow around bodies with ablative coatings," *Teplofiz. Aéromekh.*, **11**, No. 4, 501–522 (2004).
7. V. V. Kramer, "Experimental determination of coefficients of rotational derivatives by a kinematic method. Aerodynamics of unsteady motion," *Tr. TsAGI*, No. 725, 81–98 (1958).
8. N. I. Sidnyaev, V. O. Moskalenko, S. K. Kholodnov, and V. M. Ovchinnikov, "Experimental aerodynamic study of a meteo missile," *Oboron. Tekh.*, No. 1, 15–18 (1994).